International Journal of Thin Films Science and Technology

http://dx.doi.org/10.12785/ijtfst/030207

Influence of Energy Nitrogen Ion Implantation on Structural and Mechanical Properties of Chromium Thin Film

M. Manouchehrian[1,*], M. M. Larijani[2] and B. Banagar[3]
[1] *Department of Physics, South Tehran Branch, Islamic Azad University, Tehran, Iran*
[2] *Nuclear Science and Technology Research Institute (NSTRI), P. O. Box 31485-498, Karaj, Iran*
[3] *Plasma Physics Research Center, Science and Research Branch, Islamic Azad University, Tehran, Iran*

E. mail: mmojtahedfr@yahoo.com

Received: 28 Dec. 2013, Revised: 23 Feb. 2014; Accepted: 25 Feb. 2014
Published online: 1 May 2014

Abstract: Chromium thin films were deposited on 304 stainless steel using the hollow cathode discharge (HCD) method. Chromium films were implanted with nitrogen ions at different energies ((15-25-35-45) keV) and at a dose of 5×10^{17}ions/cm^2. The implanted films were characterized using x-ray diffraction (XRD), atomic force microscopy (AFM), microhardness testing, friction coefficient measurements, and wear mechanism study. The XRD results confirmed that increasing energy does not effect the formation of the CrN phase. AFM images showed that surface roughness changed proportionally to grain size after implantation. It was found that hardness increased as energy increased. From the friction coefficient measurement, it could be inferred that the friction coefficient decreased as energy increased. The wear mechanism for the un-implanted sample was abrasion, but it shifted to delamination and adhesive as energy increased.

Keywords:implantation, XRD, Abrasion, AFM, friction coefficient, microhardness

1. INTRODUCTION

In many tribological applications, metal nitride coatings are now commonly used [1]. Different techniques have been used for surface amendments such as sputtering, ion implantation and ion coating. Ion implantation is a very attractive technique for improving the surface characteristics of materials and can be used to introduce other chemical species and generate defects in target materials [2-5]. This technique is widely used to improve the surface mechanical properties of alloys containing a reactive metal such as nickel, titanium, aluminum, and chromium [6, 7]. Chromium coating is used in industry to improve wear, erosion, and corrosion properties. Nitrogen ion implantation on chromium surfaces and alloys usually improves hardness, wear resistance, and corrosion resistance. Chromium nitride coatings have been gaining popularity in recent years and are becoming important technological materials in the fields of cutting and forming tools, bearing and machine parts, dies and modulus [8]. The objective of this research was to determine the effect of nitrogen ion energy on the microstructure, surface morphology and mechanical properties of chromium thin film deposited on 304 stainless steel.

2. EXPERIMENTAL DETAILS

Chromium thin films were deposited on 304 stainless steel by hollow cathode discharge (HCD) gun model DLKD-1800 with 15kW power. The substrates were cut into 10mm×10mm×1mm slabs, and then cleaned with acetone and ethanol in an ultrasonic bath for 30 min. The vacuum chamber base pressure was 2×10^{-3}Pa. Prior to deposition, substrates were cleaned by argon ion bombardment produced in an electric discharge chamber for 30 min. The bias voltage and substrate temperature were fixed at -50V and 683K, respectively, during the deposition. The thickness of the deposited Cr layers was determined to be about 377±30nm by mechanical profilometer (DECTAK 3). Then a Kaufman ion source was used for ion implantation of the as-coated samples. The samples were implanted with nitrogen ions at different energies ((15-25-35-45) keV) with dose of 5×10^{17}ions/cm^2. The working pressure was 9×10^{-3}Pa. The implantation parameters are summarized in Table 1. The phase and crystalline structure of the samples were characterized by X-ray diffraction (XRD) using a Philips-PW 1800 with Cu K_α radiation (40kV,30mA).Scanning was conducted from 20˚ to 80° at step size 0.02˚ and 1s per step. The topography and roughness of the samples were investigated using an atomic force microscope

(Auto probe CP) on non-contact mode, a scanning velocity of 1 Hz, and a 256 pixel power resolution. Nano-indentation tests were carried out with a Berkovich tetrahedral indenter with a load 10 mN. Five indentations were taken and averaged for each sample. The hardness (H) and elastic modulus were derived according to Oliver and Parr model [9]. Friction and wear tests were performed using a pin-on-disk tribometer. A Si_3N_4 ball with a diameter of 2/2 cm was used as the counterpart. The normal loading was 3/2N, and the relative sliding speed was 0/08 m/s. The tests were carried out under atmospheric pressure at a temperature of 25C° and 50% relative humidity. Images of the wear track mechanism in the un-implanted and implanted samples with different energies were investigated by scanning electron microscopy (SEM) using a Hitachis-4160.

Table 1: The process parameters during implantation.

Sample	Energy (keV)	Fluxes (ions/cm^2)	temperature (K)
C_1	Unimplanted	-	-
C_2	15	5×10^{17}	398
C_3	25	5×10^{17}	400
C_4	35	5×10^{17}	400
C_5	45	5×10^{17}	403

3. RESULTS AND DISCUSSION

3.1 Crystal structure

Figure 1 shows the XRD patterns of un-implanted and implanted samples with nitrogen ions at different energies 15, 25, 35 and 45 keV with dose of 5×10^{17} ions/cm^2. In all XRD patterns, in addition to three peaks at 2θ=44.63º, 2θ=50.70º, and 2θ=75.00º which were related to the 304 stainless steel substrates, peaks of Cr(110) and Cr(200) with cubic structures were observed at 2θ=44.38º and 2θ=64.58º, respectively (ref. code 01-085-1335). Increasing energy does not affect the formation of the CrN phase, but depth of influence and range of distribution of nitrogen ions can change in chromium layers. If the CrN phase is formed, it will probably have an amorphous structure.

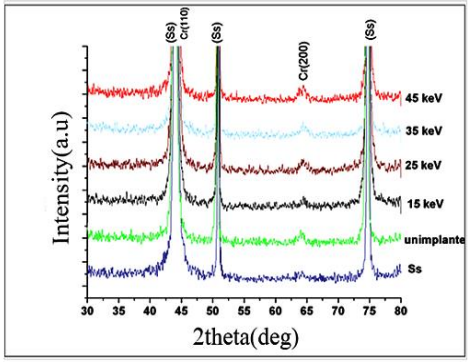

Figure 1: XRD patterns of as-coated and implanted samples with nitrogen ion.

3.2. AFM analysis

The effects of changing the energies of nitrogen ions on the microstructure of various samples are shown in Figure 2. Topography of the surface samples was analyzed by AFM, and the dimensions of the scan area were 2μm ×2μm. Figure 2 also presents the changes in grain size and sample surface shape which occurred as energy increased. Figure 2a shows the image related to as-coated sample C_1. It is obvious that the sample had a columnar structure and that grains grew in the form of a pyramid with wide peaks and are almost condensed. Images from the implanted samples are given in Figures 2(b-e). A common behavior can be seen in all images; in all samples, nano-particles grew parallel to each other, similar to prayer beads, which may be due to the presence of parallel microgrooves on the sample surface which were created while polishing. The grooves can act as active zones for nucleation and growth. In comparing images related to sample C_1(Fig. 2a) and sample C_2(Fig. 2b), it is evident that the applied energy is used to compress the grains and shrink their size through the surface diffusion of atoms. Increasing the energy in sample C_3(Fig. 2c) leads to the absorbed atoms having more mobility and caused the grains to combine with each other. The grains grow shows a hillock structure in sample C_4(Fig. 2d), and there are deep grooves between the grains because of the displacement of grain boundaries. In sample C_5(Fig. 2e) because of sputtering induced by ion bombardment, a distance between the grains appears which leads to the formation of columnar structure.

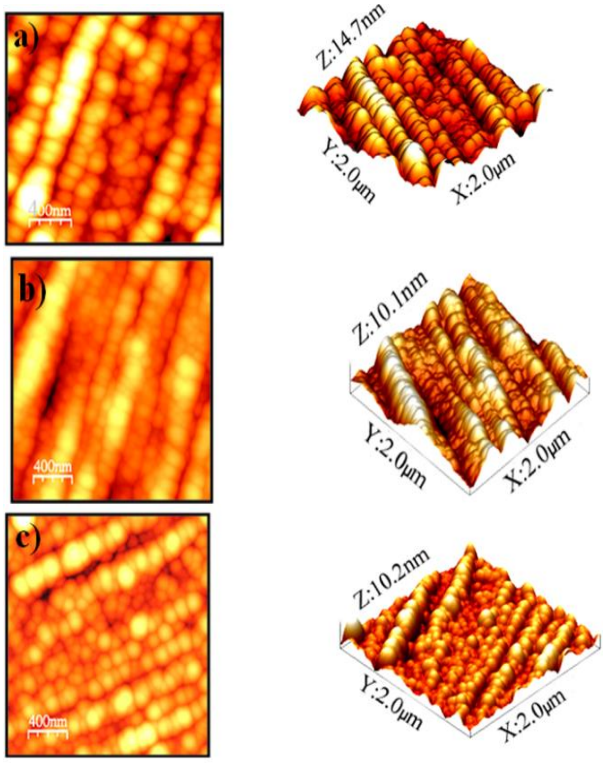

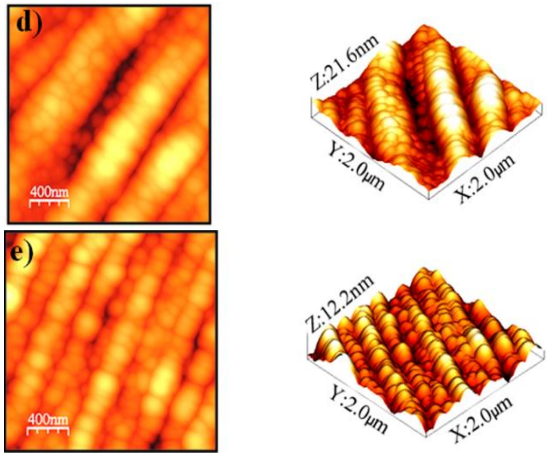

Figure 2: 2D and corresponding 3D height AFM images of as-coated and implanted samples with nitrogen ion: (a) sample c_1, (b) sample c_2, (c) sample c_3 , (d) sample c_4 and (e) sample c_5

Table 2 shows the values of average (Ra) and root mean square roughness (rms) as well as grain size for as-coated and implanted samples. It is obvious that energy increased leads to decrease of roughness, except in sample C_4 in which roughness suddenly increases by a higher rate of sputtering. However, induced stress by implantation can also influence this increase [10]. From Table 2, it can be seen that there is a direct relationship between roughness value and grain size, which is in accordance with literature [11].

Table 2: variation of average roughness and root mean square roughness as well as grain size

Sample	Surface Roughness		Grain Diameter [nm]
	rms[A°]	R_a[A°]	
C_1	15.9	12.4	150±12
C_2	15	12	143±22
C_3	9.4	7.5	138±18
C_4	28.6	23.6	134±14
C_5	14.5	11.6	132±27

3.3. Mechanical properties

3.3.1. Micro-hardness and Young's modulus

Table 3 shows the results of micro-hardness and Young's modulus for as-coated and implanted samples in 10 mN loads. It was observed that hardness and Young's modulus increases as energy increases, possibly because of the deeper penetration of nitrogen ions and the thickening of the amorphous nitride layer [12]. Overall, factors like surface roughness, ion concentration of the nitrogen, and grain size have the greatest impact on hardness and Young's modulus. According to the hardness values obtained in this study, it can be said that grain size has the strongest effect on hardness. Decreasing grain size according to the Hall-Petch equation and nitrogen sediment in the chromium layer causes increase in hardness and Young's modulus [10].

Table 3: Microhardness and Young's modulus of as-coated and implanted samples as a function of energy ion implantation.

Sample	Hardness(GPa) 10mN	Young's modulus (GPa) 10mN
C_1	5.33±0.68	223.3±9.6
C_2	5.59±0.25	253.1±5.8
C_3	5.75±0.05	255.4±1. 5
C_4	17.32±0.24	263.9±2.0
C_5	19.57±0.7	264.1±6.5

Figure 3 shows atomic force microscopic images of indentations created in the surfaces of samples C_2 and C_5 after the micro-hardness test with a 10mN load. A decrease in the indentation area was seen when energy increased from 15keV to 45keV, illustrating the increase in hardness.

Figure 3: Atomic force microscopic images of indentations created in the surfaces of samples: (a) Sample c_2 and (b) sample c_5.

3.3.2. Friction coefficient

Figure 4 shows a diagram of the friction coefficient versus distance for as-coated and implanted samples. It can be seen that the friction coefficient in implanted samples decreases in comparison with that of the as-coated samples. Generally, the friction coefficient depends on the two factors of surface roughness and hardness. Sample C_5 had the lowest friction coefficient because of its less surface roughness and more hardness compared with other samples. Scanning electron microscopy was used to study the wear mechanism.

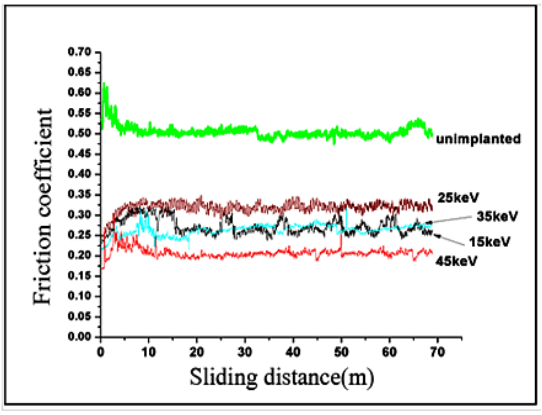

Figure 4: Friction coefficient as a function of sliding distance.

3.3.3. Wear mechanism

Wear grooves created on the surface of as-coated and implanted samples are shown in Figure 5. Fractures can be seen on the surface of sample C_1(Fig. 5a), which indicate abrasion wear in this sample, probably because of the application of high power or the brittle material forming the layer. Pitting is observed on the surface of sample C_3(Fig. 5b) which was refilled, but caused hard coarseness on the sample surface; therefore, wear in this sample is of the abrasion type. Some smashing and pitting was seen on the surface of sample C_4(Fig. 5c) which shows delamination wear. Some areas of the surface of sample C_5(Fig. 5d) were cut out and subsequently re-attached; therefore, wear is of the adhesive type. The wear mechanisms in samples C_1 and C_3 were not much different, but with increasing energy (samples C_4 and C_5), because of the mechanical work (displacement of atoms), wear types are delamination and adhesive, respectively. The surface of the sample which is undergoing nitrogen ion implantation is affected by compressive stress, and this could lead to improved wear resistance. Generally, factors which are effective in improving wear resistance are hardness increase and friction decrease, because a decrease in the friction coefficient means a decrease of transfer tangent power in the surface of the samples. Images also show that the wear track decreases as energy increases, which indicates the improvement of wear resistance.

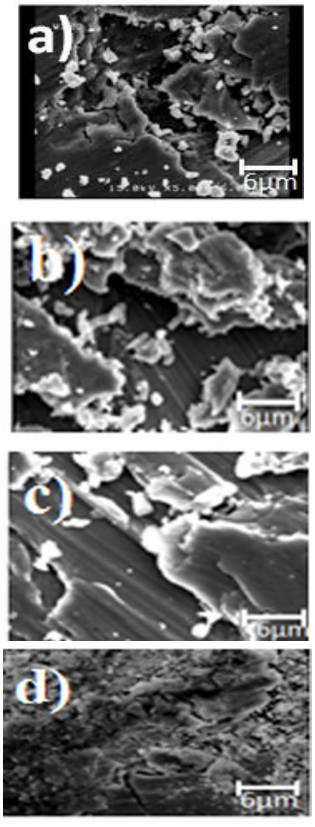

Figure 5: The morphologies of grooves wear formed. (a) sample c_1, (b) sample c_3, (c) sample c_4 and (d) sample c_4

4. CONCLUSIONS

XRD patterns showed that increasing nitrogen ion energy had no effect on forming the CrN phase, but penetration depth and diffusion domain of atoms changed. Calculating grain size by atomic force microscopic images illustrated that generally, the grain size decreased in implanted samples. Nitrogen sediment in the solid solution after the nitrogen ion implantation caused hardness to increase. Nitrogen ion implantation caused the friction coefficient to decrease. The value of decrease in vertical power ranged from 0.5 in sample C_1 to 0.23 in sample C_5. The wear mechanism for sample C_1 is abrasion, but with increased energy, the wear mechanism shifted to delamination and adhesive.

ACKNOWLEDGEMENT

In this research project "The effect of dose and nitrogen ion energy on the hardness behavior of the chromium thin film" is supported by South Tehran Branch, Islamic Azad University, Tehran, Iran.

REFERENCES

[1] G.Berg, C.Friedrich, E.Broszeit, C.Berger, Development of chromium nitride coatings substituting titanium nitride, Surf. Coat. Technol. **86-87** (1996) 184-191.

[2] F.M Kustas, W.T Misr, W.T Tack, Nitrogen implantation of type 303 stainless steel gears for improved wear and fatigue resistance, Mater. Sci. Engin. **90** (1987) 407.

[3] Y.Sugizaki, T.Yasunaga, H.Tomari, Improvement of corrosion resistance of titanium by co-implantation, Surf. Coat. Technol, **83** (1996) 167-174.

[4] B.Y Tang, K.Y Gan, P.Yang, X.F Wang, L.P Wang, S.Y Wang, P.K Chu, Surface modification of 2Cr13 oil pump steel by plasma immersion ion implantation–ion beam enhanced deposition (PIII–IBED), Thin Solid Films, **402** (2002) 211-214.

[5] L.R Shen, K.Wang, J.Tie, H.H Tong, Q.C Chen, D.L Tang, R.K.Y Fu, P.K Chu, Modification of high-chromium cast iron alloy by N and Ti ion implantation, Surf. Coat. Technol. **196** (2005) 349-352.

[6] H.Pelletier, D.Muller, P.Mille, A.Cornet, J.J Grob, Effect of high-energy implantation on TAFe titanium alloy, Surf. Coat. Technol. **151–152** (2002) 42-46.

[7] M.Fujinami, R.Suzuki, T.Ohdaira, T.Mikado, Characterization of H-related defects in H-implanted Si with slow positrons, Appl. Surf. Sci. **149** (1999) 188-192

[8] A.Kollitsch, F.Hontscol, Wear reduction by ion implantation-assisted deposition, Vaccum, **44**(1993) 291.

[9] R.Martinez, J.A Garsia, R.J Rodriguez, B.Lerga, C.Labrugere, M.Lahaye, A.Guette, Study of the tribological modifications induced by nitrogen implantation on Cr, Mo and W, Surf. Coat. Technol. **174 /175** (2003) 1253-1259.

[10] W.L Li, W.D Fei, Y.Sun, Effects of implantation conditions on the roughness of N-implanted α-Fe, Mater. Sci. Lett. **21** (2002) 239-241.

[11] K.Khojier, H.Savaloni, Nano-Structure and electrical properties of N^+ ion implanted titanium thin films as a function of N^+ ion flux, Theor. Appl. Phys. **3** (2009) 15-19.

[12] F.Caccavale, G.De Marchi, F.Gonella, P.Mazzoldi, C.Meneghini, A.Quaranta, G.W Arnold, G.Bttaglin, G.Mattei, Irradiation-induced Ag-colloid formation in ion-exchanged soda-lime glass, Nuclear Instruments and Methods in Physics Research Section B, **96** (1995) 382-385.